ELSEVIER

Engineering Analysis with Boundary Elements 24 (2000) 671–684

ENGINEERING ANALYSIS *with* BOUNDARY ELEMENTS

www.elsevier.com/locate/enganabound

Dual boundary element analysis using complex variables for potential problems with or without a degenerate boundary

J.T. Chen*, Y.W. Chen

Department of Harbor and River Engineering, Taiwan Ocean University, Keelung, Taiwan, ROC

Received 9 September 1999; received in revised form 13 April 2000; accepted 19 May 2000

Abstract

The dual boundary element method in the real domain proposed by Hong and Chen in 1988 is extended to the complex variable dual boundary element method. This novel method can simplify the calculation for a hypersingular integral, and an exact integration for the influence coefficients is obtained. In addition, the Hadamard integral formula is obtained by taking the derivative of the Cauchy integral formula. The two equations (the Cauchy and Hadamard integral formula) constitute the basis for the complex variable dual boundary integral equations. After discretizing the two equations, the complex variable dual boundary element method is implemented. In determining the influence coefficients, the residue for a single-order pole in the Cauchy formula is extended to one of higher order in the Hadamard formula. In addition, the use of a simple solution and equilibrium condition is employed to check the influence matrices. To extract the finite part in the Hadamard formula, the extended residue theorem is employed. The role of the Hadamard integral formula is examined for the boundary value problems with a degenerate boundary. Finally, some numerical examples, including the potential flow with a sheet pile and the torsion problem for a cracked bar, are considered to verify the validity of the proposed formulation. The results are compared with those of real dual BEM and analytical solutions where available. A good agreement is obtained.

Keywords: Complex-variable BEM; Dual BEM; Degenerate boundary; Cauchy integral formula and Hadamard integral formula

1. Introduction

For scalar or vector potential problems, the analyst may encounter problems with a singularity; nevertheless, the singular behavior is often ignored in numerical methods in the expectation that the error will be limited to the vicinity of the singularity. However, it is essential for the employed formulation to be capable of describing the singular behavior when the singularity arises from a degenerate boundary, for example, the sheetpile design in seepage problems where the singularity dominates the force exerted on the sheet piles as shown in Fig. 1 [1], and in the determination of the stress intensity factor for a cracked bar under torsion in fracture mechanics as shown in Fig. 2 [2], where the strength of the singularity is the very value to be sought. Mathematically speaking, the two problems have a degenerate boundary. In this regard, it may be recalled that an insurmountable difficulty in the use of conventional BEM crack (sheetpile) modeling stems from a mathematical degeneracy in the BEM formulation when both upper and lower crack (sheetpile) surfaces lie in the same location. The equations for the points at the upper surface of the crack (sheetpile) are dependent on and even identical to those at the lower, and, as a consequence, the formulation is insufficient to secure a unique solution. Undeniably, it results in an infinite number of solutions. In a numerical calculation, this is evident in a vanishing determinant or algebraic singularity of the coefficient matrix of the discretized equations. In the finite element approach, to tackle the degenerate boundary problems, special treatments, such as the quarter point rule, have been used, or special singular or hybrid elements have been developed. For examples, MSC/NASTRAN provides the capabilities of singular CRAC3D and CRAC2D elements for crack problems, but for the potential problems with a singularity, no counterparts have been developed for the above-mentioned commercial program to the authors' knowledge [1,3].

In recent decades, the boundary element method has evolved into be a widely accepted tool as a solution for the engineering problems. The easy data preparation due to the one-dimension reduction, compared to the FEM, makes it attractive for practical use. However, for problems with singularity arising from a degenerate boundary, it is well known that the coincidence of the boundaries gives rise to an ill-conditioned problem. The subdomain technique

* Corresponding author. Fax: +886-2-2463-2932.
E-mail address: jtchen@ind.ntou.edu.tw (J.T. Chen).

0955-7997/00/$ - see front matter
PII: S0955-7997(00)00025-4

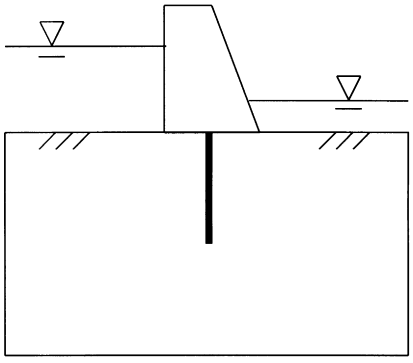

Fig. 1. Classical problem of seepage flow with a sheet pile under a dam.

with artificial boundaries has been introduced to ensure a unique solution for the Laplace equation [4] and Navier equation [5], respectively. The main drawback of the technique is that the deployment of artificial boundaries is arbitrary and, thus, cannot be implemented easily in an automatic procedure. In addition, the model creation is much more troublesome than in the single-domain approach. To tackle such degenerate boundary problems, dual integral formulations have been proposed, e.g. for potential/seepage/Darcy flows around cutoff walls/sheetpiles [6], for crack problems [7–12], for screen impinging in acoustics [2,13–17], and for thin air foils in aerodynamics [18]. Using the dual integral formulations, all the aforementioned boundary value problems can be made well posed and can be solved efficiently in the original single domain. A review article on dual BEM can be found in Ref. [19]. However, all the above formulations were done in the real domain. Owing to the difficulty in calculating the Hadamard principal value that requires much effort to solve; another approach is desired [21]. The complex variable boundary element method (CVBEM) has been developed to solve potential problems [20]. For example, applications in aerodynamics [22], elasticity [23], corner problem [24], plate [25], external flow [26] and torsion bar [27] can be easily found. All the above mentioned papers focus on problems with a nondegenerate boundary. For such problems, the

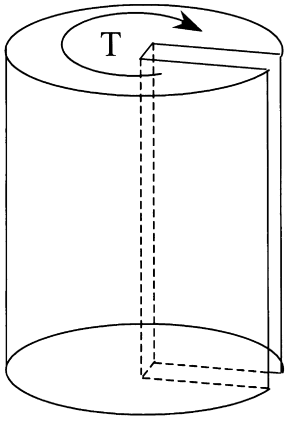

Fig. 2. Classical problem of torsion problem for a cracked bar.

Cauchy integral formula constructs the integral representation for the solution of the primary field. The irregular integrals can be more easily determined in the complex domain than in the real domain. However, two disadvatanges will occur if only the Cauchy integral formula is employed in the CVBEM. One is in transforming the boundary conditions [28], and the other is the limitation of applications to problems with a degenerate boundary. After differentiation, the Hadamard integral formula can represent the solution for the secondary field and can overcome the two disadvantages for the conventional CVBEM.

In this paper, the complex variable dual boundary element method based on the formulation of the dual integral equations is employed by constructing the Hadamard integral formula from the derivative of the Cauchy integral formula. This avoids both the above mentioned two disadvantages. A constant element scheme is used, and the closed-form formulas for the influence coefficients are determined. The general purpose program CVDBEM (Complex Variable Dual Boundary Element Method) was developed to analyze the seepage flow under a dam with sheetpiles and torsion problems for a cracked bar. Several examples are furnished, and the boundary element solutions are compared with results obtained using real dual BEM and analytical solutions where available. Also, the rank deficiency obtained using the equations in the real and the imaginary parts is investigated using the singular value decomposition technique. This technique is employed to solve the overdeterminated system of the matrix. The boundary effect is also discussed in this paper.

2. Dual integral formulation in the complex domain

In this study, we focus on boundary value problems for scalar potential. The governing equation and boundary conditions are shown below. The governing equation

$$\nabla^2 u(x,y) = 0, \quad (x,y) \text{ in } D, \tag{1}$$

where D is the domain and the boundary conditions are

$$u(x,y) = \bar{u}, \quad (x,y) \text{ on } B_u \tag{2}$$

$$\frac{\partial u(x,y)}{\partial n} = \bar{t}, \quad (x,y) \text{ on } B_t, \tag{3}$$

in which u is the potential, B_u the boundary with Dirichlet data, B_t the boundary with Neumann data, and n is the outnormal direction on the boundary and $B = B_u + B_t$.

In order to extend the problem solvable in the domain of a real variable to one solvable in the domain of a complex variable, we construct a complex function, $w(z)$, from $u(x,y)$ by means of

$$w(z) = u(x,y) + \mathrm{i}v(x,y), \tag{4}$$

where $z = x + \mathrm{i}y$ is a complex variable and $\mathrm{i}^2 = -1$.

By the Cauchy integral formula [29], we have

$$2\pi \mathrm{i} w(z) = \int_B \frac{w(t)}{(t-z)} \mathrm{d}t, \quad z \in D, \tag{5}$$

where B is the considered boundary. By differentiating Eq. (5) with respect to z, we obtain [30,31]

$$2\pi \mathrm{i} w'(z) = \int_B \frac{w(t)}{(t-z)^2} \mathrm{d}t, \quad z \in D. \tag{6}$$

Eqs. (5) and (6) are termed the dual complex variable boundary integral equations for domain points, which are different from those of the real variable case [32] as follows:

$$2\pi u(\mathbf{x}) = \int_B \{T(\mathbf{s},\mathbf{x})u(\mathbf{s}) - U(\mathbf{s},\mathbf{x})t(s)\} \, \mathrm{d}B(\mathbf{s}), \quad \mathbf{x} \in D \tag{7}$$

$$2\pi t(\mathbf{x}) = \int_B \{M(\mathbf{s},\mathbf{x})u(\mathbf{s}) - L(\mathbf{s},\mathbf{x})t(s)\} \, \mathrm{d}B(\mathbf{s}), \quad \mathbf{x} \in D, \tag{8}$$

where $t = \partial u/\partial n$, $U(\mathbf{s},\mathbf{x})$, $T(\mathbf{s},\mathbf{x})$, $L(\mathbf{s},\mathbf{x})$ and $M(\mathbf{s},\mathbf{x})$ are the four kernel functions. By moving the point z to the boundary, we can derive the dual complex variable boundary integral equations for boundary points as follows [33]:

$$\pi \mathrm{i} w(z) = \mathrm{CPV} \int_B \frac{w(t)}{(t-z)} \mathrm{d}t, \quad z \in B \tag{9}$$

$$\pi \mathrm{i} w'(z) = \mathrm{HPV} \int_B \frac{w(t)}{(t-z)^2} \mathrm{d}t, \quad z \in B, \tag{10}$$

where CPV and HPV are the Cauchy and the Hadamard principal values, respectively. The definitions of CPV and HPV in the complex domain are similar to those in the real case of dual boundary integral equations as follows:

$$\pi u(\mathbf{x}) = \mathrm{CPV} \int_B T(\mathbf{s},\mathbf{x})u(\mathbf{s}) \, \mathrm{d}B(\mathbf{s}) - \int_B U(\mathbf{s},\mathbf{x})t(\mathbf{s}) \, \mathrm{d}B(\mathbf{s}), \quad \mathbf{x} \in B \tag{11}$$

$$\pi t(\mathbf{x}) = \mathrm{HPV} \int_B M(\mathbf{s},\mathbf{x})u(\mathbf{s}) \, \mathrm{d}B(\mathbf{s}) - \mathrm{CPV} \int_B L(\mathbf{s},\mathbf{x})t(\mathbf{s}) \, \mathrm{d}B(\mathbf{s}), \quad \mathbf{x} \in B. \tag{12}$$

By choosing the equation for the real part in Eq. (5), we have

$$2\pi u(x) = \int_B \frac{\partial\{\ln(r)\}}{\partial n} u(s) \, \mathrm{d}B(s) - \int_B \frac{\partial\{\ln(r)\}}{\partial t} v(s) \, \mathrm{d}B(s), \tag{13}$$

where $\partial/\partial n$ denotes the normal derivative and $\partial/\partial t$ is the tangential derivative. By integrating by parts for the second term on the right-hand side of the equal sign and employing the Cauchy–Rieman equations as follows:

$$\frac{\partial v}{\partial t} = \frac{\partial u}{\partial n} \tag{14}$$

$$-\frac{\partial v}{\partial n} = \frac{\partial u}{\partial t}, \tag{15}$$

we can derive Eq. (7) in the real dual model. Similarly, $v(x, y)$ also satisfies the same integral equations since u and v are both harmonic functions. In the case of problems with boundary conditions of the Neumann type, it is necessary to construct the representation for the normal flux, t, in terms of a complex formulation. Using the following relations for the real part and imaginary part for $w'(z)$:

$$\mathrm{Re}\{w'(z)\} = \frac{\partial u}{\partial x} \tag{16}$$

$$\mathrm{Im}\{w'(z)\} = -\frac{\partial u}{\partial y}, \tag{17}$$

we have the alternative form for the second equation in the dual model as

$$t = \mathrm{Re}(w'(z))n_1 - \mathrm{Im}(w'(z))n_2, \tag{18}$$

where $w'(z)$ can be obtained from Eq. (10), and $\mathrm{Re}\{\cdot\}$ and $\mathrm{Im}\{\cdot\}$ denote the real part and imaginary part, respectively.

3. Discretization of the complex dual boundary integral equations

Using the constant element scheme for $w(z)$ along boundary B, we can discretize Eqs. (9) and (10) in the following forms:

$$\pi \mathrm{i} w(z_p) = \int_B \frac{w(t)}{(t-z_p)} \mathrm{d}t = \sum_{q=1}^{N} \int_{B_q} \frac{1}{(t_q - z_p)} \mathrm{d}t_q w(t_q) \tag{19}$$

$$\pi \mathrm{i} w'(z_p) = \int_B \frac{w(t)}{(t-z_p)^2} \mathrm{d}t = \sum_{q=1}^{N} \int_{B_q} \frac{1}{(t_q - z_p)^2} \mathrm{d}t_q w(t_q), \tag{20}$$

where B_q is the qth boundary element and N denotes the number of boundary elements. The influence coefficients can be defined as

$$C_{pq}^1 \equiv \int_{B_q} \frac{1}{(t_q - z_p)} \mathrm{d}t_q \tag{21}$$

$$C_{pq}^2 \equiv \int_{B_q} \frac{1}{(t_q - z_p)^2} \mathrm{d}t_q. \tag{22}$$

For the regular element, no singularity occurs, and the closed-form integral formula can be obtained as follows:

$$\int_{B_q} \frac{1}{(t_q - z_p)} \mathrm{d}t_q = \ln(t_q - z_p)\Big|_{t_q = t_q^1}^{t_q = t_q^2} \tag{23}$$

$$\int_{B_q} \frac{1}{(t_q - z_p)^2} \mathrm{d}t_q = \frac{-1}{(t_q - z_p)}\Big|_{t_q = t_q^1}^{t_q = t_q^2}, \tag{24}$$

where the selected branch cut does not intersect the considered domain, t_q^1 and t_q^2 are the two end points for the qth

boundary element. For the singular and hypersingular integrals, we derive the Cauchy principal value and Hadamard principal value using the surrounding technique as follows:

$$\mathrm{CPV}\int_{B_q}\frac{1}{(t_q-z_p)}\mathrm{d}t_q=0 \tag{25}$$

$$\mathrm{HPV}\int_{B_q}\frac{1}{(t_q-z_p)^2}\mathrm{d}t_q=\mathrm{CPV}\int_{B_q}\frac{1}{(t_q-z_p)}\mathrm{d}t_q-\frac{2}{\varepsilon}, \tag{26}$$

where CPV and HPV are defined as

$$\mathrm{CPV}\int_B\frac{f(t)}{(t-z)}\mathrm{d}t=\lim_{\varepsilon\to 0}\int_{B-B_\varepsilon}\frac{f(t)}{t-z}\mathrm{d}t \tag{27}$$

$$\begin{aligned}\mathrm{HPV}\int_B\frac{f(t)}{(t-z)^2}\mathrm{d}t&=\frac{\mathrm{d}}{\mathrm{d}z}\left\{\int_{B-B_\varepsilon}\frac{f(t)}{t-z}\mathrm{d}t\right\}\\&=\lim_{\varepsilon\to 0}\left\{\int_{B-B_\varepsilon}\frac{f(t)}{(t-z)^2}\mathrm{d}t-\frac{2}{\varepsilon}f(z)\right\}\end{aligned} \tag{28}$$

in which B_ε is small detour path and the last term,

$$-\frac{2}{\varepsilon}f(z)$$

comes from the Leibnitz differentiation.

After discretizing Eq. (9), we have

$$\begin{bmatrix} C_{pq}^{1\mathrm{R}} & \vdots & -C_{pq}^{1\mathrm{I}} \\ \cdots & & \cdots \\ C_{pq}^{1\mathrm{I}} & \vdots & C_{pq}^{1\mathrm{R}} \end{bmatrix}_{2N\times 2N}\begin{Bmatrix} u_q \\ \cdots \\ v_q \end{Bmatrix}_{2N\times 1}=\begin{Bmatrix} 0 \\ \cdots \\ 0 \end{Bmatrix}_{2N\times 1,} \tag{29}$$

where

$$C_{pq}^{1}=\mathrm{CPV}\int_{B_q}\frac{1}{(t_q-z_p)}\mathrm{d}t_q-\pi\mathrm{i}\delta_{pq} \tag{30}$$

$$C_{pq}^{1\mathrm{R}}=\mathrm{Re}[C_{pq}^{1}] \tag{31}$$

$$C_{pq}^{1\mathrm{I}}=\mathrm{Im}[C_{pq}^{1}], \tag{32}$$

in which $\delta_{pq}=1$ if $p=q$; otherwise is zero. In a similar way, Eq. (18) can be discretized to get the following algebraic equation:

$$\begin{aligned}&[(n_1C_{pq}^{2\mathrm{R}}-n_2C_{pq}^{2\mathrm{I}})\vdots-(n_1C_{pq}^{2\mathrm{I}}+n_2C_{pq}^{2\mathrm{R}})]_{N\times 2N}\begin{Bmatrix} u_q \\ \cdots \\ u_q \end{Bmatrix}_{2N\times 1}\\&\quad=\{\pi\mathrm{i}t_p\}_{N\times 1},\end{aligned} \tag{33}$$

where

$$C_{pq}^{2}=\mathrm{HPV}\int_{B_q}\frac{1}{(t_q-z_p)^2}\mathrm{d}t_q \tag{34}$$

$$C_{pq}^{2\mathrm{R}}=\mathrm{Re}[C_{pq}^{2}] \tag{35}$$

$$C_{pq}^{2\mathrm{I}}=\mathrm{Im}[C_{pq}^{2}]. \tag{36}$$

After constructing the linear algebraic Eqs. (29) and (33), we can assemble them into the following form:

$$\begin{aligned}&\begin{bmatrix} C_{pq}^{1\mathrm{R}} & \vdots & -C_{pq}^{1\mathrm{I}} \\ \cdots & & \cdots \\ C_{pq}^{1\mathrm{I}} & \vdots & C_{pq}^{1\mathrm{R}} \\ \cdots & & \cdots \\ (n_1C_{pq}^{2\mathrm{R}}-n_2C_{pq}^{2\mathrm{I}}) & \vdots & -(n_1C_{pq}^{2\mathrm{I}}+n_2C_{pq}^{2\mathrm{R}}) \end{bmatrix}_{3N\times 2N}\begin{Bmatrix} u_q \\ \cdots \\ v_q \end{Bmatrix}_{2N\times 1}\\&=\begin{Bmatrix} 0 \\ \cdots \\ 0 \\ \cdots \\ t_p\pi\mathrm{i} \end{Bmatrix}_{3N\times 1.}\end{aligned} \tag{37}$$

Substituting the known boundary conditions of u and t, we have

$$[A]\{x\}=\{y\}, \tag{38}$$

where $[A]$ is the assembled matrix, $\{x\}$ is the unknown vector, and $\{y\}$ is the known vector derived from the boundary conditions. Since the complex formulation is considered, Eq. (38) is overdeterminated. The least squares method or SVD technique can be employed to solve the overdeterminated algebraic equation (38).

4. Use of a simple solution and a test of the equilibrium condition

Since a constant potential can be a solution for $w(z)$, we have the solution

$$w(z)=c_1+c_2\mathrm{i} \tag{39}$$

$$t=0. \tag{40}$$

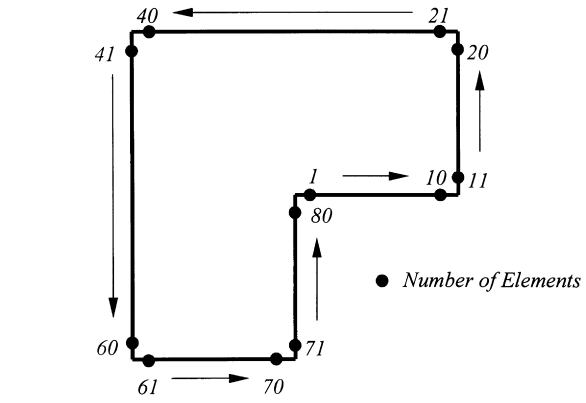

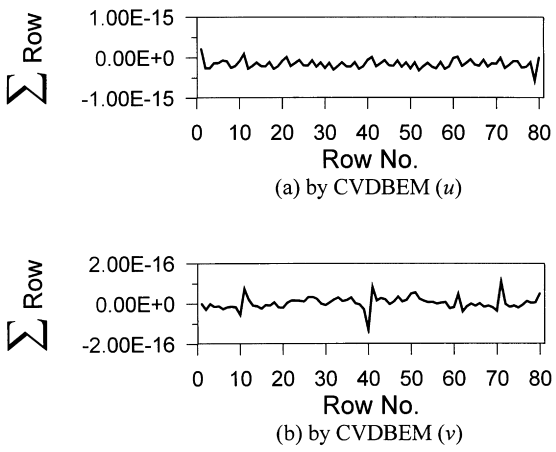

Fig. 3. The sum of each row in the influence matrix.

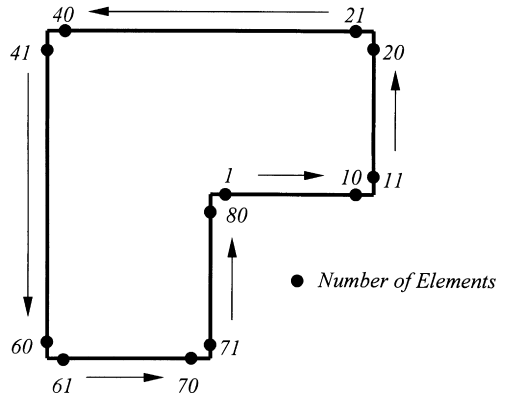

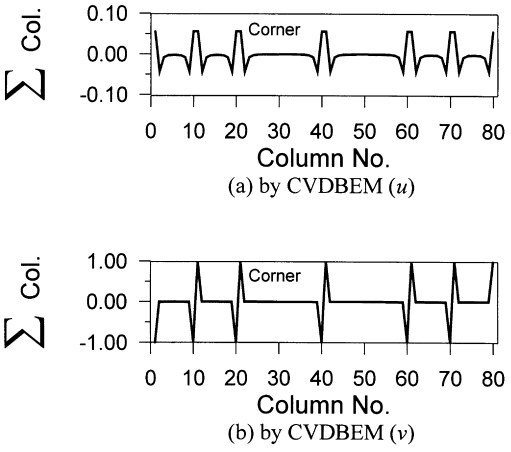

Fig. 4. The sum of each column in the influence matrix.

Substituting Eqs. (39) and (40) into Eq. (37), we have

$$\begin{bmatrix} C_{pq}^{1R} & \vdots & -C_{pq}^{1I} \\ \cdots & & \cdots \\ C_{pq}^{1I} & \vdots & C_{pq}^{1R} \\ \cdots & & \cdots \\ (n_1 C_{pq}^{2R} - n_2 C_{pq}^{2I}) & \vdots & -(n_1 C_{pq}^{2I} + n_2 C_{pq}^{2R}) \end{bmatrix}_{3N\times 2N} \begin{Bmatrix} c_1 \\ \cdots \\ c_2 \end{Bmatrix}_{2N\times 1} = \begin{Bmatrix} 0 \\ \cdots \\ 0 \\ \cdots \\ 0 \end{Bmatrix}_{3N\times 1.} \tag{41}$$

Since c_1 and c_2 can be arbitrary, the four matrices,

$$[C_{pq}^{1R}],\ [C_{pq}^{1I}],\ [n_1 C_{pq}^{2R} - n_2 C_{pq}^{2I}],$$

and

$$[-(n_1 C_{pq}^{2I} + n_2 C_{pq}^{2R})],$$

all have eigenvalues of zero and eigenvectors of $\{1\cdots 1\cdots 1\}_{N\times 1.}$ In other words, the rank of the four matrices must be equal to or smaller than $N-1$, and the sum of all the elements in each row for the four matrices is zero. Fig. 3 shows that almost a zero value can be obtained for

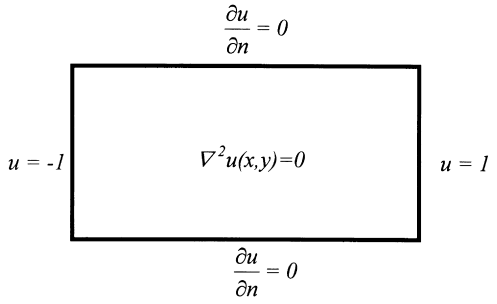

Fig. 5. Flow without a degenerate boundary.

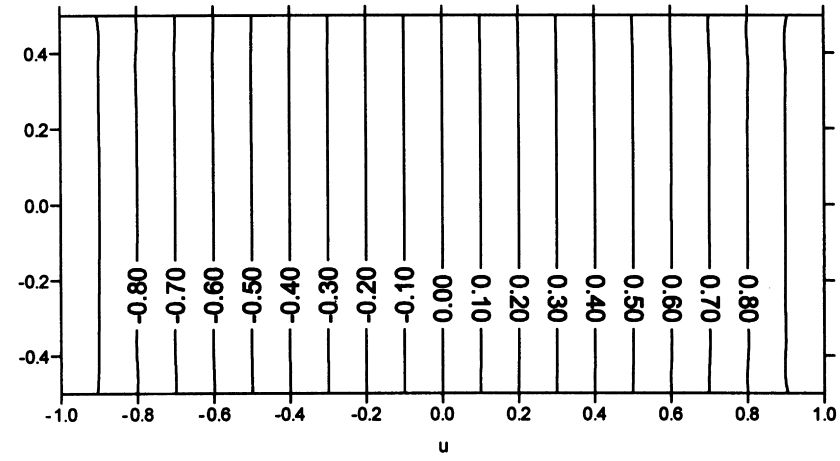

(a)

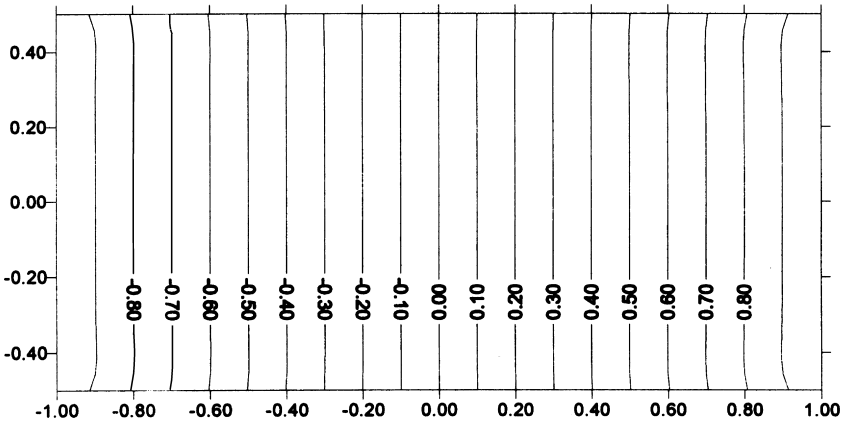

(b)

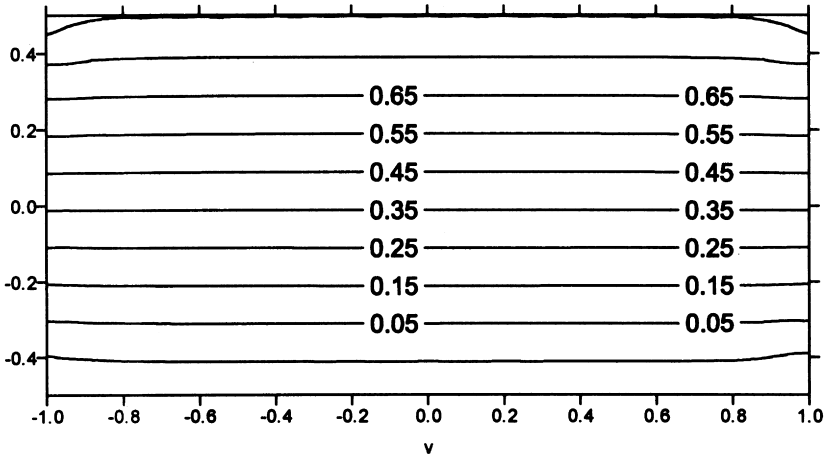

(c)

Fig. 6. Potential distribution for Case 1: (a) *u* field by complex dual BEM; (b) *u* field by real dual BEM; (c) *v* field by complex dual BEM.

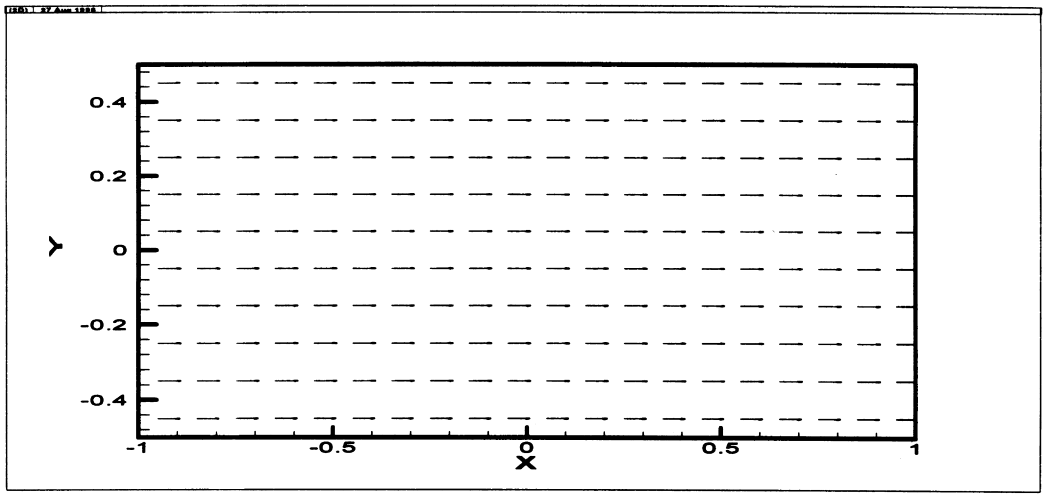

(a)

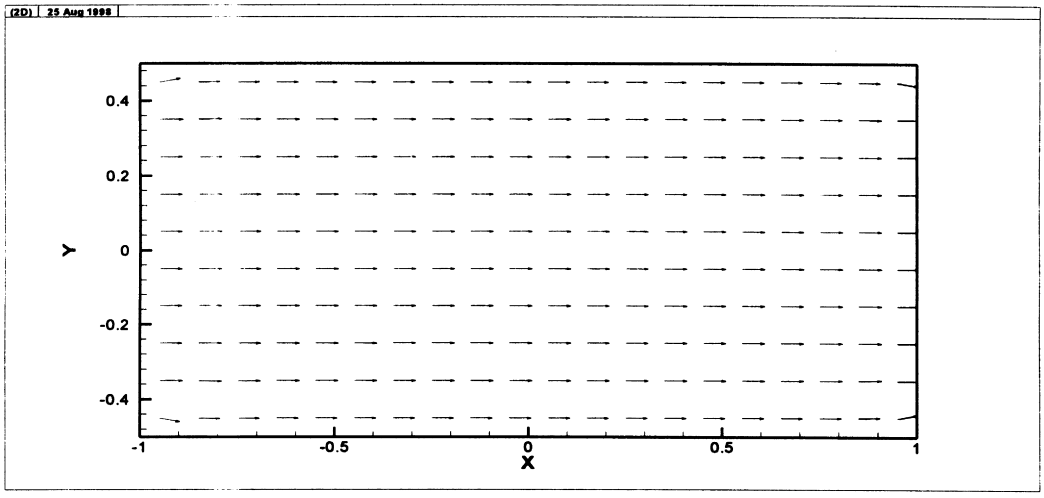

(b)

Fig. 7. Velocity distribution for Case 1: (a) real dual BEM solution; (b) complex dual BEM solution.

the L-shape potential problem of Case 2, which will be elaborated later.

If the length of all the elements are equal, the equilibrium condition should be satisfied as follows:

$$\int_B t(s)\,\mathrm{d}B(s) = 0. \tag{42}$$

After substituting the t_p in Eq. (33) into Eq. (42), we find that the sums of each column in the two matrices

$$[n_1 C_{pq}^{2\mathrm{R}} - n_2 C_{pq}^{2\mathrm{I}}] \text{ and } [-(n_1 C_{pq}^{2\mathrm{I}} + n_2 C_{pq}^{2\mathrm{R}})],$$

are zero theoretically. Since the BEM is derived from the energy form instead of the equilibrium equation, some numerical errors will be present when the test of the equilibrium condition is used. It is found that a large residual of the equilibrium condition in Eq. (42) appears near the corner in an L shape as shown in Fig. 4, where the numerical errors in the solution are usually very large. This index provides a guideline for obtaining a better solution by employing the adaptive mesh [34,35].

5. On the rank of the influence matrices

For problems without a degenerate boundary, we have the

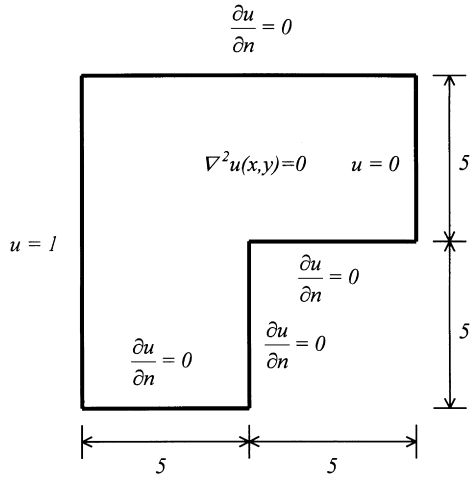

Fig. 8. Flow without a degenerate boundary and with an L-shaped corner singularity.

ranks for the following eight matrices:

$$\text{rank}[C_{pq}^{1R}] = N - 1 \tag{43}$$

$$\text{rank}[C_{pq}^{1I}] = N - 1 \tag{44}$$

$$\text{rank}\left[\begin{array}{c|c} C_{pq}^{1R} & -C_{pq}^{1I} \end{array}\right]_{N\times 2N} = N \tag{45}$$

$$\text{rank}\left[\begin{array}{c|c} C_{pq}^{1I} & C_{pq}^{1R} \end{array}\right]_{N\times 2N} = N \tag{46}$$

$$\text{rank}\begin{bmatrix} C_{pq}^{1R} \\ \cdots \\ C_{pq}^{1I} \end{bmatrix}_{2N\times N} = 2N \tag{47}$$

$$\text{rank}\begin{bmatrix} -C_{pq}^{1I} \\ \cdots \\ C_{pq}^{1R} \end{bmatrix}_{2N\times N} = 2N \tag{48}$$

$$\text{rank}\left[\begin{array}{c|c} C_{pq}^{1R} & -C_{pq}^{1I} \\ \cdots & \cdots \\ C_{pq}^{1I} & C_{pq}^{1R} \end{array}\right]_{2N\times 2N} = 2N - 2 \tag{49}$$

$$\text{rank}\left[\begin{array}{c|c} C_{pq}^{1R} & -C_{pq}^{1I} \\ \cdots & \cdots \\ C_{pq}^{1I} & C_{pq}^{1R} \\ \cdots & \cdots \\ (n_1 C_{pq}^{2R} - n_2 C_{pq}^{2I}) & -(n_1 C_{pq}^{2I} + n_2 C_{pq}^{2R}) \end{array}\right]_{3N\times 2N} = 2N, \tag{50}$$

where N is the number of boundary elements.

For problems with a degenerate boundary, we have more dependent rows since the constraint equations obtained by

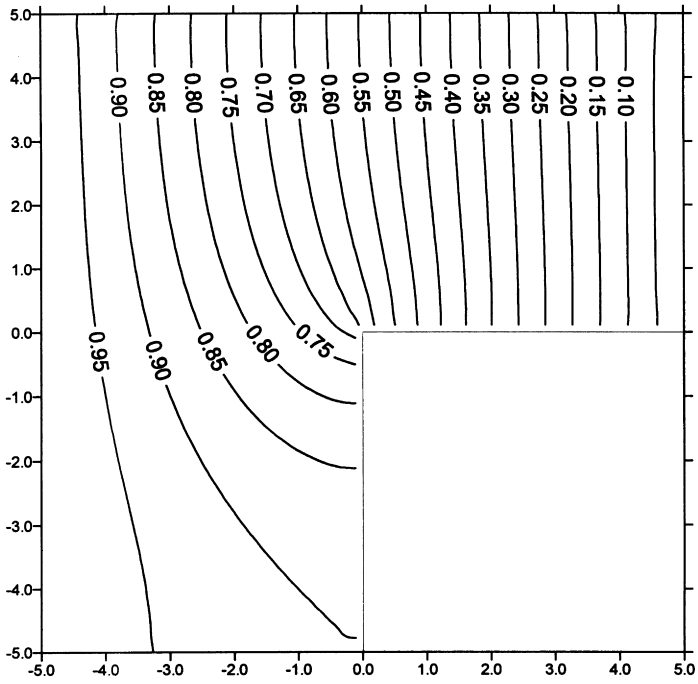

Fig. 9. Potential distribution for Case 2.

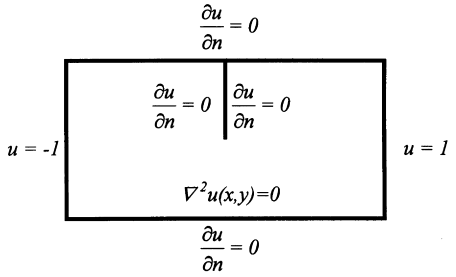

Fig. 10. Flow with a degenerate boundary of a sheetpile.

collocating the points on the both sides of the degenerate boundary are the same. To obtain sufficient constraint equations, Eq. (18) plays an important role in the dual CVBEM.

6. Numerical results and discussions

6.1. Case 1: flow without a degenerate boundary

The governing equation and boundary conditions are shown in Fig. 5. The exact solution is

$$u(x_1, x_2) = x_1. \tag{51}$$

Based on the CVDUAL program, the potential distribution is shown in Fig. 6(a) for u field. For comparison, the u is also solved by using real dual BEM (BEPO2D program) [1] and is shown in Fig. 6(b). Good consistency can be obtained except in the corner. The imaginary part, v field, by the complex dual BEM is also shown in Fig. 6(c). The velocity distribution is shown in Fig. 7(a) and (b) using the real and complex dual BEM, respectively. The velocity gradients in Fig. 7(b) are directly determined according to Eq. (18) rather than through the numerical differentiation in the conventional CVBEM [20].

6.2. Case 2: flow without a degenerate boundary but with a L-shaped corner singularity

The governing equation and boundary conditions in the L-shaped domain are shown in Fig. 8. The potential distribution is shown in Fig. 9 and compares well with those in Ref. [36]. Also, the results of the sums in the rows and columns for the influence matrices, obtained using a simple

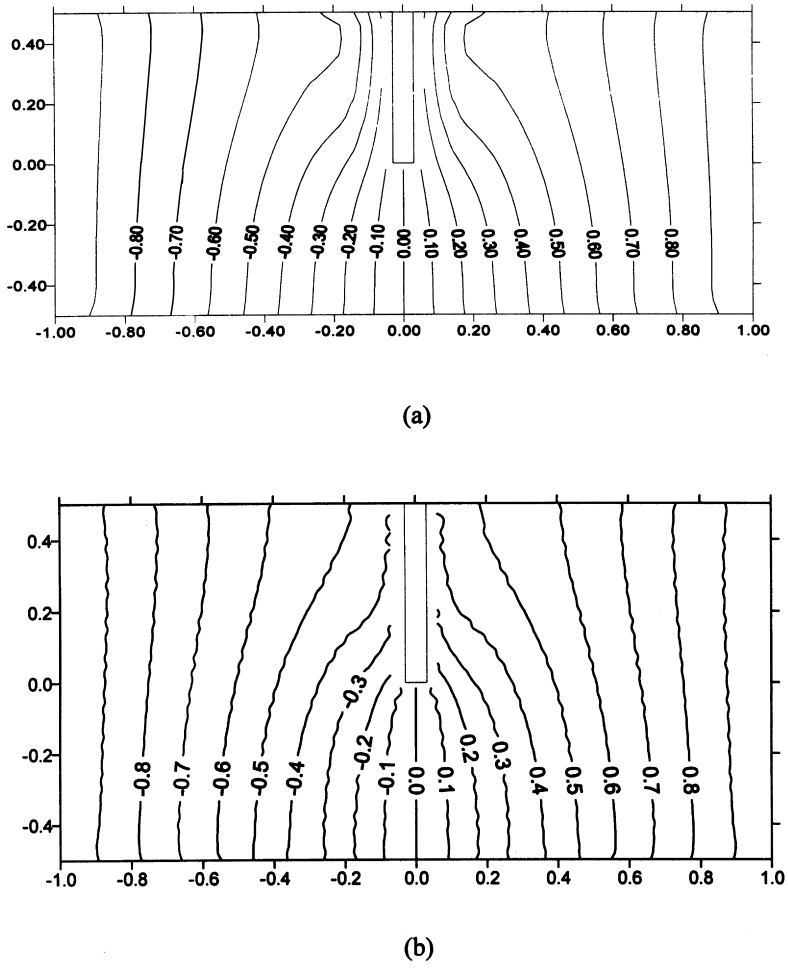

Fig. 11. Potential distribution for Case 3: (a) real dual BEM solution; (b) complex dual BEM solution.

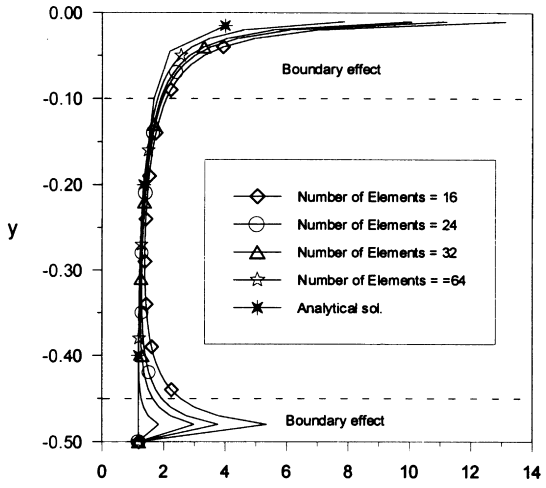

Fig. 12. Potential gradient in the *x* direction beneath the sheetpile for Case 3.

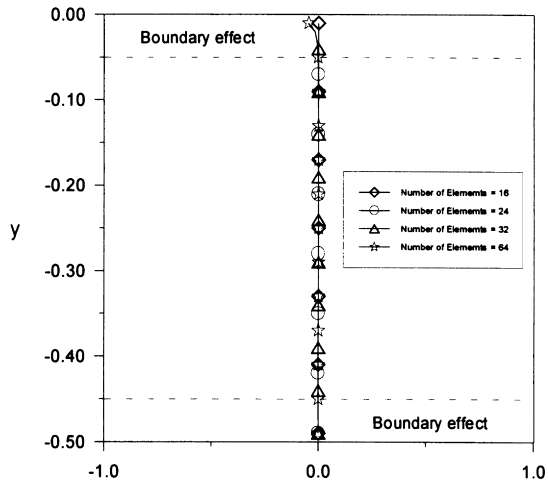

Fig. 13. Potential gradient in the *y* direction beneath the sheetpile for Case 3.

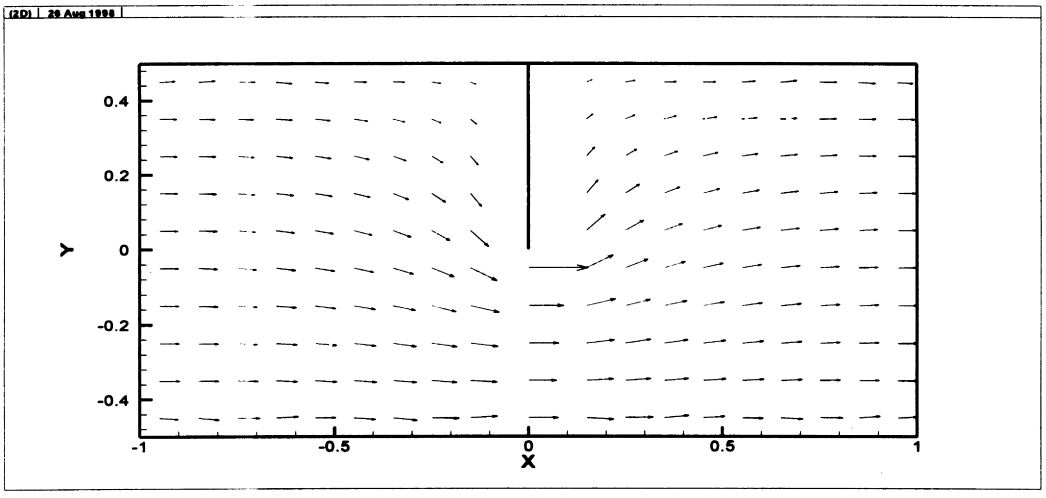

(a)

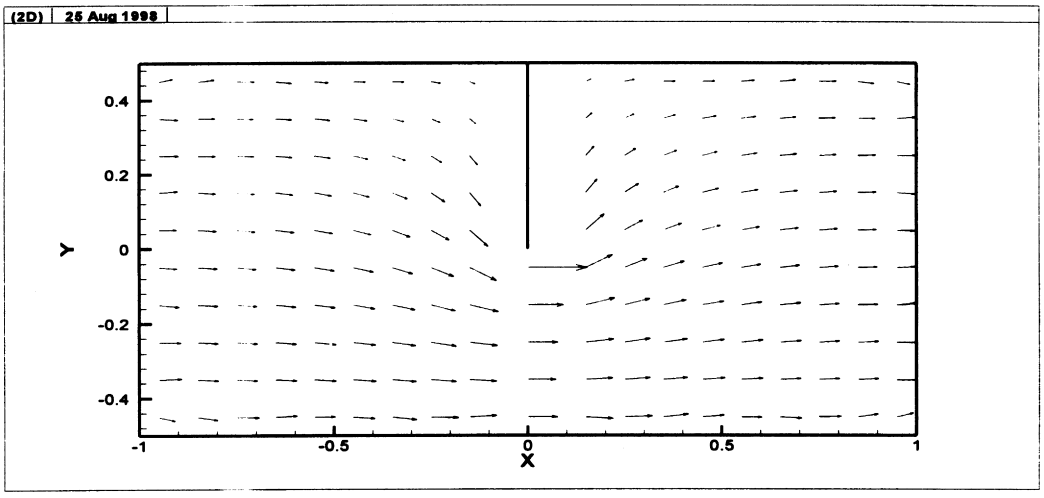

(b)

Fig. 14. Velocity distribution for Case 3: (a) real dual BEM solution; (b) complex dual BEM solution.

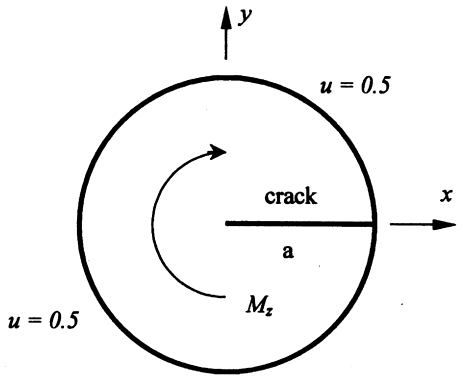

Fig. 15. Torsion problem for a cracked bar.

solution and the equilibrium condition, respectively, are shown to be near zero in Figs. 3 and 4.

6.3. Case 3: flow with a degenerate boundary of a sheetpile

Cases 1 and 2 are problems without a degenerate boundary. For problems with a degenerate boundary, the conventional CVBEM fails, and the dual approach is employed to obtain a unique solution. In the following two cases, a degenerate boundary is present. Case 3 is the flow field with a sheetpile. The governing equation and boundary conditions are shown in Fig. 10. Eq. (37) in conjunction with the singular value decomposition technique is employed to enable the overdeterminated matrix to have a pseudo-inverse. The potential distribution is shown in Fig. 11(a) and (b) by using the real and complex dual BEM, respectively.

The difference between them cannot be distinguished easily by naked eyes except for the results near the boundary. The velocities in the x-direction and the y-direction beneath the sheetpile are shown in Figs. 12 and 13, respectively. The boundary effect for the velocity shown in the figures occurs in the same way if the real dual BEM is used. Moreover, the analytical solution obtained using the Christoffel transformation in Ref. [4] and the results obtained using the real dual BEM are both compared with the present solution. The velocity distribution is shown in Fig. 14(a) and (b) by using the real and complex dual BEM, respectively. A good agreement is thus found.

6.4. Case 4: torsion problem with a degenerate boundary of crack

For the Saint–Venant torsion problem of a cracked bar, the governing equation and boundary conditions for the potential can be formulated as shown in Fig. 15. The analytical solution in polar coordinates can be found in Ref. [37]

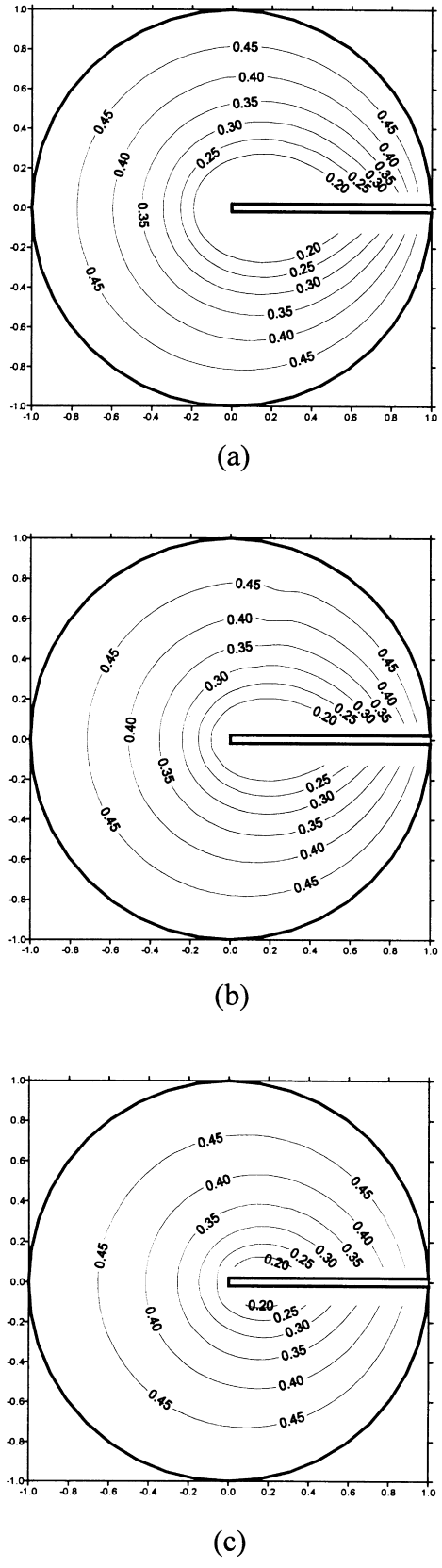

Fig. 16. Potential distribution for Case 4: (a) complex dual BEM solution; (b) exact solution; (c) real dual BEM solution.

Table 1
Comparisons of real dual BEM and complex dual BEM

Domain	Real [32]	Complex
State	$u(x_1, x_2)$	$w(z) = u(x_1, x_2) + \mathrm{i}v(x_1, x_2)$
Governing equation	$\nabla^2 u(x_1, x_2) = 0$	$\nabla^2 w = 0$
Dirichlet BC	$u = \bar{u}$	$u = \mathrm{Re}\{w(z)\} = \bar{u}$
Neumann BC	$t = \dfrac{\partial u}{\partial n} = \bar{t}$	$t = \mathrm{Re}\{w'(z)\}n_1 - \mathrm{Im}\{w'(z)\}n_2 = \bar{t}$
Dual boundary integral equations for domain points	$2\pi u(x) = \int_B T(s,x)u(s)\,\mathrm{d}B(s) - \int_B U(s,x)t(s)\,\mathrm{d}B(s)$	$w(z) = \dfrac{1}{2\pi\mathrm{i}}\int_B \dfrac{w(t)}{(t-z)}\mathrm{d}t$
	$2\pi t(x) = \int_B M(s,x)u(s)\,\mathrm{d}B(s) - \int_B L(s,x)t(s)\,\mathrm{d}B(s)$	$w'(z) = \dfrac{1}{2\pi\mathrm{i}}\int_B \dfrac{w(t)}{(t-z)^2}\mathrm{d}t$
Dual boundary integral equations for boundary points	$\pi u(x) = \mathrm{CPV}\int_B T(s,x)u(s)\,\mathrm{d}B(s) - \int_B U(s,x)t(s)\,\mathrm{d}B(s)$	$w(z) = \dfrac{1}{\pi\mathrm{i}}\mathrm{CPV}\int_B \dfrac{w(t)}{(t-z)}\mathrm{d}t$
	$\pi t(x) = \mathrm{HPV}\int_B M(s,x)u(s)\,\mathrm{d}B(s) - \mathrm{CPV}\int_B L(s,x)t(s)\,\mathrm{d}B(s)$	$w'(z) = \dfrac{1}{\pi\mathrm{i}}\mathrm{HPV}\int_B \dfrac{w(t)}{(t-z)^2}\mathrm{d}t$
Matrix from	$T\tilde{u} = U\tilde{t}$	$[C^1]\begin{Bmatrix}\tilde{u}\\ \tilde{v}\end{Bmatrix} = \{0\}$
	$M\tilde{u} = L\tilde{t}$	$[C^2]\begin{Bmatrix}\tilde{u}\\ \tilde{v}\end{Bmatrix} = \{\tilde{t}\}$
Linear algebraic equation	$Ax = y$	$Ax = y$

and is shown below:

$$u(r,\phi) = 32\frac{a^2}{\pi}\sum_{n=0}^{\infty}\frac{\left(\frac{r}{a}\right)^{(2n+1)/2} - \left(\frac{r}{a}\right)^2}{(2n+1)[16-(2n+1)^2]} \times \sin\frac{(2n+1)\phi}{2} + \frac{r^2}{2}, \tag{52}$$

where (r, ϕ) is the polar coordinate, a the crack length, and the diameter of the torsion bar is 2 cm. The potential distribution obtained using the complex dual BEM is shown in Fig. 16(a) and compares well with the exact solution shown in Fig. 16(b) obtained using Eq. (52). In addition, the results obtained using the real dual BEM are shown in Fig. 16(c) for comparison (Table 1). Table 2 indicates that the complex-variable BEM results are better than those of real-variable BEM after comparing the exact solution. It is also found that the error near the crack tip is larger than that of other region.

7. Conclusions

The dual integral formulation in the domain of a complex variable has been presented here. It has been confirmed that the developed program, CVDUAL,

Table 2
Potential values of $u(x,0)$, $-1 < x < 0$ using complex dual BEM and real dual BEM

Position (x, y)	Analytical solution	CDBEM (error, %)	RDBEM (error, %)
(0.0, 0.0)	0.0000	0.0000 (0.0)	0.0000 (0.0)
(−0.1, 0.0)	0.2037	0.1008 (50.5)	0.3110 (52.7)
(−0.2, 0.0)	0.2764	0.2070 (25.1)	0.3549 (28.4)
(−0.3, 0.0)	0.3267	0.2753 (15.7)	0.3867 (18.4)
(−0.4, 0.0)	0.3654	0.3263 (10.7)	0.4119 (12.7)
(−0.5, 0.0)	0.3969	0.3672 (7.5)	0.4326 (9.0)
(−0.6, 0.0)	0.4235	0.4014 (5.2)	0.4501 (6.3)
(−0.7, 0.0)	0.4463	0.4306 (3.5)	0.4653 (4.2)
(−0.8, 0.0)	0.4663	0.4561 (2.2)	0.4786 (2.6)
(−0.9, 0.0)	0.4841	0.4787 (1.1)	0.4904 (1.3)
(−1.0, 0.0)	0.5000	0.5000 (0.0)	0.5000 (0.0)

is acceptable through comparison with the analytical solution and real dual BEM. The hypersingularity in the domain of a complex variable can be easily determined for problems with a degenerate boundary. It has been found that the BEM in the context of the present formulation is particularly suitable for the problems with singularity arising from a degenerate boundary. For a potential problem with singularity, dual BEMs (real or complex) are superior to FEM not only in terms of data preparation but also in terms of accuracy. In engineering practice, since model creation requires the greatest amount of effort, the present dual BEM, which avoids the development of an artificial boundary, is strongly recommended for industrial applications.

Acknowledgements

Support from the National Science Council, Taiwan, under Grant NSC 87-2211-E-019-017 is gratefully acknowledged. The authors also gratefully thank Prof. H.-K. Hong of the National Taiwan University for helpful discussions and Prof. A.H.D. Cheng of the University of Deleware for providing the analytical solution for the potential flow with a sheetpile.

References

[1] Chen JT, Hong H-K, Chyuan SW. Boundary element analysis and design in seepage problems using dual integral formulation. Finite Elements in Analysis and Design 1994; 17(1):1–20.
[2] Chen JT, Chen KH, Yeih W, Shieh NC. Dual boundary element analysis for cracked bars under torsion. Engineering Computations 1998;15(6):732–49.
[3] Chen JT, Lin SL, Chiou CY, Chyuan SW, Hwang JY, Harn WR, Chin WT. Finite element analysis and engineering applications using MSC/NASTRAN. Taipei, Taiwan: Northern Gate Publishers, 1996 (in Chinese).
[4] Lafe OE, Montes JS, Cheng AHD, Liggett JA, Liu PL-F. Singularity in Darcy flow through porous media. J Hydra Div, ASCE 1980;106(6):977–97.
[5] Blandford GE, Ingraffea AR, Liggett. Two-dimensional stress intensity fator computation using the boundary element method. Int J Num Meth Engng 1981;17:387–404.
[6] Chen JT, Hong H-K. Singularity in Darcy flow around a cutoff wall. In: Brebbia CA, Conner JJ, editors. Advances in Boundary Elements, Field and Flow Solution, vol. 2. 1989. p. 15–27.
[7] Hong H-K, Chen JT. Derivations of integral equations of elasticity. J ASCE 1988;144(6):1028–44 (Em5).
[8] Hong H-K, Chen JT. Generality and special cases of dual integral equations of elasticity. J CSME 1988;9(1):1–19.
[9] Portela A, Aliabadi MH, Rooke DP. The dual boundary element method: effective implementation for crack problems. Int J Num Meth Engng 1992;33:1269–87.
[10] Mi Y, Aliabadi MH. Dual boundary element method for three-dimensional fracture mechanics analysis. Eng Anal Bound Elem 1992;10:161–71.
[11] Gray LJ. Boundary element method for regions with thin internal cavities. Engng Anal Bound Elem 1989;6(4):180–4.
[12] Martin PA, Rizzo FJ, Gonsalves IR. On hypersingular integral equations for certain problems in mechanics. Mech Res Commun 1989;16(2):65–71.
[13] Chen JT, Chen KH. Dual integral formulation for determining the acoustic modes of a two-dimensional cavity with a degenerate boundary. Engng Anal Bound Elem 1998;21(2):105–16.
[14] Chen KH, Chen JT, Liou DY. Dual boundary element analysis for a acoustic cavity with an incomplete partition. Chin J Mech 1998;14(2):1–11 (in Chinese).
[15] Chen JT, Wong FC. Dual formulation of multiple reciprocity method for the acoustic mode of a cavity with a thin partition. J Sound Vib 1998;217(1):75–95.
[16] Chen JT, Chen KH, Chyuan SW. Numerical experiments for acoustic modes of a square cavity using the dual BEM. Appl Acoustics 1999;57(4):293–325.
[17] Chen JT. Recent development of dual BEM in acoustic problems. Keynote lecture. In: Onate E, Idelsohn SR, editors. Proceedings of the Fourth World Congress on Computational Mechanics, Argentina, 1998. p. 106.
[18] Wang CS, Chu S, Chen JT. Boundary element method for predicting store airloads during its carriage and separation procedures. In: Grilli, editor. Computational engineering with boundary elements, Fluid and Potential Problems, vol. 1. CMP, 1990.
[19] Chen JT, Hong H-K. Review of dual boundary element methods with emphasis on hypersingular integral and divergent series. Appl Mech Rev, ASME 1999;52(1):17–33.
[20] Hromadka TV, Lai C. The complex variable boundary element method in engineering analysis. New York: Springer, 1987.
[21] Hui CY, Mukherjee S. Evaluation of hypersingular integrals in the boundary element method by complex variable techniques. Int J Solids Struct 1997;34(2):203–21.
[22] Storti M, D'Elia J, Idelsohn SR. CVBEM Formulation for multiple profiles and cascades. Appl Mech Rev, ASME 1995;48(11): 203–10.
[23] Linkov AM, Mogilevskaya SG. Complex hypersingular integrals and integral equations in elasticity. Acta Mechanica 1994;105: 189–205.
[24] Kolhe R, Ye W, Hui CY, Mukherjee S. Complex variable functions for usual and hypersingular integral equations for potential problems with applications to corners and cracks. Comput Mech 1996;17:279–86.
[25] Gu L, Huang MK. A complex variable boundary element method for solving plane and plate problems of elasticity. Engng Anal Bound Elem 1991;8(6):266–72.
[26] Mokry M. Complex variable boundary element method for external potential flows. AIAA J 1991;29(12):207–8.
[27] Chou SI, Shamas-Ahmadi M. Complex variable boundary element method for torsion of hollow shafts. Nucl Engng Anal Design 1992;136:255–63.
[28] Yu GQ, Rasmussen TC. Application on the ordinary least-squares approach for solution of complex variable boundary element problems. Int J Numer Meth Engng 1997;40:1281–93.
[29] Churchill RV, Brown JW. Complex variables and applications. 5th ed. New York: McGraw-Hill, 1990.
[30] Gakhov F. Boundary value problems. Oxford: Pergamon, 1966.
[31] Hromadka II TV, Whitley RJ. Advances in the complex variable boundary element method. Berlin: Springer, 1998.
[32] Chen JT, Hong H-K. Boundary element method. 2nd ed. Taipei, Taiwan: New World Press, 1992 (in Chinese).
[33] Chen YW. Complex variable dual boundary element method. Master Thesis, Department of Harbor and River Engineering, Taiwan Ocean University, Keelung, Taiwan, 1998.

[34] Chen JT, Hong H-K. Dual boundary integral equations at a corner using contour approach around singularity. Adv Engng Software 1994;21(3):169–78.
[35] Liang MT, Chen JT, Yang SS. Error estimation for boundary element method. Engng Anal Bound Elem 1999;23(3):257–65.
[36] Jaswon MA, Symm GT. Integral equation methods in potential theory and elastostatics. London: Academic, 1977.
[37] Lebedev NN, Skalskaya IP, Ulfyans YS. Worked problems in applied mathematics. Translated by Silverman RA. New York: Dover, 1965. p. 185–92.